Modeling of Diffusion-Controlled Reactions in Free Radical Solution and Bulk Polymerization: Model Validation by DSC Experiments

Dimitris S. Achilias, George D. Verros

Laboratory of Organic Chemical Technology, Department of Chemistry, Aristotle University of Thessaloniki, Thessaloniki GR-54124, Greece

Received 26 June 2009; accepted 21 October 2009
DOI 10.1002/app.31675
Published online 7 January 2010 in Wiley InterScience (www.interscience.wiley.com).

ABSTRACT: In this work, a detailed experimental study of diffusion-controlled reactions in free radical polymerization by using differential scanning calorimetry (DSC) was carried out. The systems studied include the methyl methacrylate bulk polymerization as well as the solution and the bulk polymerization of vinyl acetate at a wide range of experimental conditions including initial initiator concentration, reaction temperature, and type and amount of solvent. The conversion data obtained by DSC was successfully simulated by using a mathematical model based on sound principles such as the free volume theory. The estimated parameters, by fitting predictions of this model to conversion data obtained by DSC were found to be in close agreement with the reported parameters in the literature, thus validating both the experimental and theoretical methods used in this work. © 2010 Wiley Periodicals, Inc. J Appl Polym Sci 116: 1842–1856, 2010

Key words: radical polymerization; differential scanning calorimetry; modeling; diffusion-controlled; poly(methyl methacrylate); poly(vinyl acetate)

INTRODUCTION

The industrial importance of diffusion-controlled reactions at high conversion in free radical polymerization has led to numerous experimental and theoretical studies.[1] These diffusion-controlled reactions include termination reactions (gel effect), initiation of primary radicals (cage effect), and the propagation reaction (glass effect). The authors developed a comprehensive mathematical model for these diffusion-controlled reactions in free radical polymerization in previous works[2–5] by taking into account the diffusion phenomena in the existence of both linear and branched chains in the solution. The developed model was based on sound principles of free volume theory to account the complex phenomena appearing in the diffusion-controlled reactions and it was tested in our previous work[1–5] against the conversion and molecular weight data obtained by several workers in the field.[6–8] More specifically, the developed model was tested against the experimental data for the bulk polymerization of methyl methacrylate (MMA) obtained by Balke and Hamielec[6] and for the solution polymerization of vinyl acetate in t-butyl alcohol from Chatterjee et al.[7] and in toluene from McKenna and Villanueva.[8]

It is well known that a reliable model should be based on precise experimental data. Therefore, the aim of this work is to complete our previous studies[1–5] by further validating the developed model against conversion data obtained by carefully performed DSC experiments over a wide range of experimental conditions. DSC is a very sensitive and precise technique for measurement of the polymerization rate as a function of time, by monitoring the rate at which energy (heat) is released from the polymerizing sample. One of the greatest advantages of this method is that it provides a direct measure of the instantaneous reaction rate rather than conversion. The degree of monomer conversion (in terms of double bond conversion) is calculated by integrating the area between the DSC thermograms and the baseline established by extrapolation from the trace produced after complete polymerization (no change in the heat produced during the reaction). This process is inherently more accurate than evaluating rates from the slope of the conversion curve. In addition, the final conversion can be calculated, together with the maximum polymerization rate and the time taken to achieve it. Measurements can be easily carried out in a variety of experimental conditions including reaction temperature, initial initiator concentration, type of initiator used, and monomer(s) chemical structure. The DSC has been an especially useful tool when applied in studies of the gel-effect (autoacceleration) as well as in crosslinking reactions. Calorimetry is also well

Correspondence to: D. S. Achilias (axilias@chem.auth.gr).

established method for the online control of polymerization reactors.[9-18]

This work is structured as follows: In the following section, the experimental procedures are described in detail. In the theoretical section, the free radical reaction mechanism is briefly outlined along with the mathematical model (model equations and model parameters) for the MMA bulk polymerization as well as the free radical polymerization of vinyl acetate in both bulk and solution. Finally, results are discussed and conclusions are drawn.

EXPERIMENTAL PART

Materials

The initiator used was 2,2′-azo-bis-isobutyronitrile (AIBN) (Akzo Chemie Ltd) and it was recrystallized twice from methanol. The monomers used were methyl methacrylate (MMA) and vinyl acetate (VAc) obtained by Aldrich and they contained hydroquinone. To remove the inhibitor, the monomers were passed at least twice through a disposable packing bed column obtained from Aldrich and stored in the refrigerator until used. The monomers were also degassed immediately before polymerization.

Procedure

Polymerization was investigated using the DSC, Pyris 1 (from Perkin-Elmer) equipped with the Pyris software for windows. Indium was used for the enthalpy and temperature calibration of the instrument. Isothermal polymerizations were carried out at different temperatures, circulating oxygen-free nitrogen in the DSC cell outside the pans to avoid atmospheric oxygen getting into the sample. The reaction temperature was recorded and maintained constant (within ± 0.01°C) during the whole conversion range. Reaction mixtures were prepared by weighing the appropriate amount of initiator and dissolving it into the monomer. Samples of these solutions were placed in aluminum Perkin-Elmer sample pans, accurately weighed (10 to 20 mg), sealed, and then placed in the instrument.

The reaction exotherm (in normalized values, W/g) was recorded at a constant temperature as a function of time. The rate of heat release ($d(\Delta H)/dt$, W/g) measured by the DSC was directly converted into the overall reaction rate (dX/dt, s^{-1}) using the following formula:

$$R_p = \frac{dX}{dt} = \frac{1}{\Delta H_T}\frac{d(\Delta H)}{dt} \quad (1)$$

In which ΔH_T [J/g] denotes the total reaction enthalpy released from the reaction of all double bonds in the monomer molecule and is calculated from the product of the number of double bonds per monomer molecule ($n = 1$) times the standard heat of polymerization of a methacrylate double bond ($\Delta H_0 = 54.9$ kJ/mol) or in general of the monomer studied double bond (i.e. $\Delta H_{VAc} = 88$ kJ/mol) over the monomer molecular weight, i.e., $\Delta H_T = n\,\Delta H_0/MW_m$.

The polymerization enthalpy and conversion were calculated by integrating the area between the DSC thermograms and the baseline established by extrapolation from the trace produced after complete polymerization (no change in the heat produced during the reaction). The residual monomer content and the total reaction enthalpy can be determined by heating the sample from the polymerization temperature to 180°C at a rate of 10 K/min. The sum of enthalpies of the isothermal plus the dynamic experiment was the total reaction enthalpy. On completion of polymerization the pans were weighed again and only in a few cases a negligible loss of monomer (less than 0.2 mg) was observed.

All the experimental results reported in the following section were taken from an average of at least two experiments.

Measurements

Gel permeation chromatography

The molecular weight distribution and the average molecular weights of the PMMA products were determined by GPC. The instrument used was from Polymer Laboratories and included a pump (Marathon III HPLC pump), an Evaporative Mass Detector (PL-EMD 950), and a Plgel 5 μ MIXED-D column. All samples were dissolved in THF at a constant concentration of 0.2 wt %. After filtration of samples, 25 μL of each sample was injected into the chromatograph. The elution solvent was also THF at a constant flow rate of 1 mL/min. Calibration of GPC was carried out with standard polystyrene samples (Polymer Laboratories) by using the universal calibration technique.

THEORETICAL PART

Kinetic mechanism-mass balances

The generalized kinetic mechanism of free radical-polymerization includes initiation, propagation and termination reactions, chain transfer to monomer or solvent, and long chain branching formation by transfer to polymer and terminal double bond propagation.[5,7,8,19–25] These steps are listed as follows:

Initiation

$$I \xrightarrow{k_d} 2PR^*$$

$$PR^* + M \xrightarrow{k_I} P_{1,0}$$

Transfer to initiator reaction

$$A^* + I \xrightarrow{k_r} \text{inactive products}$$

Propagation

$$P_{n,b} + M \xrightarrow{k_p} P_{n+1,b}$$

$$P^{=}_{n,b} + M \xrightarrow{k_p} P^{=}_{n+1,b}$$

Chain transfer to monomer

$$P_{n,b} + M \xrightarrow{k_{tm}} D_{n,b} + M^*$$

$$P^{=}_{n,b} + M \xrightarrow{k_{tm}} D^{=}_{n,b} + M^*$$

$$M^* + M \xrightarrow{k_{pm}} P^{=}_{1,0}(\text{reinitiation})$$

Chain transfer to solvent

$$P_{n,b} + S \xrightarrow{k_{ts}} D_{n,b} + S^*$$

$$P^{=}_{n,b} + S \xrightarrow{k_{ts}} D^{=}_{n,b} + S^*$$

$$S^* + M \xrightarrow{k_{pm}} P_{1,0}(\text{reinitiation})$$

Chain transfer to polymer

$$P_{n,b} + D_{r,q} \xrightarrow{k_{tp}} P_{r,q+1} + D_{n,b}$$

$$P^{=}_{n,b} + D_{r,q} \xrightarrow{k_{tp}} P_{r,q+1} + D^{=}_{n,b}$$

$$P_{n,b} + D^{=}_{r,q} \xrightarrow{k_{tp}} P^{=}_{r,q+1} + D_{n,b}$$

$$P^{=}_{n,b} + D^{=}_{r,q} \xrightarrow{k_{tp}} P^{=}_{r,q+1} + D^{=}_{n,b}$$

Terminal double bond propagation

$$P_{n,b} + D^{=}_{r,q} \xrightarrow{k_{db}} P_{n+r,b+q+1}$$

$$P^{=}_{n,b} + d^{=}_{r,q} \xrightarrow{k_{db}} P^{=}_{n+r,b+q+1}$$

Termination by combination

$$P_{n,b} + P_{r,q} \xrightarrow{k_{tc}} D_{n+r,b+q}$$

$$P^{=}_{n,b} + P_{r,q} \xrightarrow{k_{tc}} D^{=}_{n+r,b+q}$$

$$P_{n,b} + P^{=}_{r,q} \xrightarrow{k_{tc}} D^{=}_{n+r,b+q}$$

$$P^{=}_{n,b} + P^{=}_{r,q} \xrightarrow{k_{tc}} D^{=}_{n+r,b+q}$$

Termination by disproportionation

$$P_{n,b} + P_{r,q} \xrightarrow{k_{td}} \frac{1}{2}D^{=}_{n,b} + \frac{1}{2}D_{n,b} + \frac{1}{2}D^{=}_{r,q} + \frac{1}{2}D_{r,q}$$

$$P^{=}_{n,b} + P_{r,q} \xrightarrow{k_{td}} D^{=}_{n,b} + \frac{1}{2}D^{=}_{r,q} + \frac{1}{2}D_{r,q}$$

$$P_{n,b} + P^{=}_{r,q} \xrightarrow{k_{td}} \frac{1}{2}D^{=}_{n,b} + \frac{1}{2}D_{n,b} + D^{=}_{r,q}$$

$$P^{=}_{n,b} + P^{=}_{r,q} \xrightarrow{k_{td}} D^{=}_{n,b} + D^{=}_{r,q}$$

All symbols used are explained in the "Nomenclature" section.

It was found convenient in this work to include a transfer to initiator reaction in the aforementioned mechanism. The species A* responsible for transfer to initiator reaction were assumed to be produced by the transfer to solvent reaction in the case of solution polymerization or by transfer to monomer in the case of bulk polymerization. More specifically, it is assumed that the initiator species decompose in a "cage" before fast reacting with the monomer M or the solvent S. Since there is not any stirring during the DSC experiments, one could anticipate that all reactants accumulate near the "cage" of initiator due to absence of convection thus causing minimal dispersion of the reactants in the bulk of the reactor. In other words, it is assumed that this accumulation near the cage of various reactants (oligomers, etc.) produced by transfer to solvent or monomer reactions causes deactivation of the initiator.

On the basis of the aforementioned reaction mechanism, one could derive mass balances assuming that the DSC capsule is an isothermal batch reactor (BR). The main mass balances used in this work are summarized as follows:

Initiator

$$\frac{1}{V}\frac{d(VI)}{dt} = -k_d I - k_r A^* I \tag{2}$$

Species A*

$$\frac{1}{V}\frac{d(VA^*)}{dt} = k_{ty} P_{00} Y;\ \text{Y : M or S} \tag{3}$$

Monomer- fractional monomer conversion (X)

$$\frac{1}{V}\frac{d(VM)}{dt} = -(k_p + 2k_{tm})MP_{00} - k_{ts}SP_{00} - k_1 PR^* M;$$
$$X = \frac{(M_0 V_0 - MV)}{M_0 V_0} \tag{4}$$

Solvent

$$\frac{1}{V}\frac{d(VS)}{dt} = -k_{ts} P_{00} S \tag{5}$$

Concentration of live radicals

$$\frac{1}{V}\frac{d(VP_{00})}{dt} = 2fk_d I - k_t P_{00}^2;\ \ P_{00} = P_{0l} + P_{0br} \tag{6}$$

All symbols are explained in the "Nomenclature" section.

A detailed description of the mass balance equations and the method of moments used to evaluate averages of the polymer molecular weight distribution can be found in previous publications from our group.[4,5,19]

Modeling diffusion-controlled reactions

The diffusion-controlled reactions at high conversion include the termination reaction (gel-effect), the primary radical initiation (cage-effect), and the propagation reaction (glass-effect).

It is assumed that the reactants inside the DSC capsule were uniformly dispersed. Under these conditions a macroscopically isothermal homogenous (absence of temperature or concentration gradients) solution or homogenous gel could be assumed. Therefore, diffusion is described by self-diffusion coefficients.

Model development closely follows our previous studies[2–5] and is summarized in the following equations

Gel effect—Residual termination

The key point in this analysis, is the overall kinetic rate constant ($k_t = k_{tc} + k_{td}$), which is written in terms of the linear termination rate constant, k_{tl} and the branched termination rate constant, k_{tbr} as well as the total concentration of "live" branched and linear radicals, P_{0b} and P_{0l}, respectively [eq. (7)]. Each of these termination rate constants is further analyzed in two terms: one accounting for the "live" radicals diffusion limitations ($k_{te,j}$; $j = l$ or br) and the other standing for the residual termination, $k_{t,reac}$, [eq. (8)].

Overall termination kinetic rate constant

$$k_t = (k_{tb}P_{0b} + k_{tl}P_{0l})/P_{00} \tag{7}$$

Termination kinetic rate constants for linear and branched radicals

$$k_{tl} = k_{te,l} + k_{t,reac};\ k_{tb} = k_{te,br} + k_{t,reac} \tag{8}$$

Following most workers in the field as recently reviewed by Achilias,[1] it is assumed in this work that the residual termination rate constant ($k_{t,reac}$) is proportional to the frequency of monomer addition to the radical chain end.

$$k_{t,reac} = A_r k_p M \tag{9}$$

The "live" radicals-diffusion termination kinetic rate constants ($k_{te,b}$, $k_{te,ln}$) were calculated by using the Smoluchowski equation:

$$\frac{1}{k_{te,j}} = \frac{1}{k_{t0}} + \frac{1}{4\pi N_A r_t \overline{D}_{p,j}} = \frac{1}{k_{t0}} + \frac{r_t^2 P_{0j}}{3\overline{D}_{p,j}};\ \ \mathrm{j = l\ or\ br} \tag{10}$$

k_{t0} stands for the total intrinsic termination rate constant ($k_{t0} = k_{tc0} + k_{td0}$) defined at zero conversion and involving two short chains, D_{pb} and D_{pl} represent the self-diffusion coefficient of "live" branched and linear macro-radicals, respectively, and are given by the following equations using the free volume theory.

$$\overline{D}_{p,l} = (D_{p0}/\overline{X}_{lr}^{\,2})\exp\lfloor -\gamma(\omega_m V_m^* + \omega_s V_s^* \xi_{23} + \omega_p V_p^* \xi_{13})/(V_F \xi_{13})\rfloor \tag{11}$$

$$\overline{D}_{p,br} = D'_{p0}\left(e^{-a\overline{X}_b}\right)\exp\lfloor -\gamma(\omega_m V_m^* + \omega_s V_s^* \xi_{23} + \omega_p V_p^* \xi_{13})/(V_F \xi_{13})\rfloor \tag{12}$$

the free volume of the mixture is given by

$$V_F/\gamma = \sum_{i=1}^{3} \frac{K_{1i}}{\gamma}(k_{2i} - T_{gi} + T)\omega_i \tag{13}$$

the symbol r_t represents the effective reaction radius for the termination reaction calculated by the excess chain end mobility theory.[1–5]

$$r_t = \left\{\ln\left[1000\tau^3 \Big/ \left(N_A \lambda_{00}^{T} \pi^{3/2}\right)\right]\right\}^{0.5} \Big/ \tau;$$
$$\tau = \left(3/2 j_c \delta^2\right)^{0.5} \tag{14}$$

δ can be measured experimentally and j_c is equal to the average number of monomer units in a dangling chain and it could be written in terms of the critical degree of polymerization for entanglement of pure polymer, x_{c0} and the volume fraction of polymer φ_p

$$j_c^{-1} = j_{c0}^{-1} + 2\varphi_p/x_{c0} \tag{15}$$

j_{c0} is a critical value corresponding to zero conversion.

The "live" radicals concentration (P_{0l} and P_{0b}) as well as the number average degree of polymerization ($\overline{X}_{lr}$, $\overline{X}_b$) of "live" radicals can be directly calculated by using the method of moments as shown in our previous work.[5]

Finally, the cage effect and the glass effect in this work are considered according to our previous studies.[1–4]

Cage effect

$$\frac{1}{f} = \frac{1}{f_0} + E\frac{r_2^3}{3r_1}\frac{k_{p0}}{f_0}\frac{(M)}{D_I} \tag{16}$$

TABLE I
Model Parameters for the VAc Polymerization

A. Kinetic rate constants for the VAc polymerization[23–25]

$k_d = 4.5 \times 10^{14}$ exp(-30000/RT) for AIBN [s^{-1}]

$k_{p0} = 7 \times 10^7$ exp(-6300/RT) [L mol^{-1} s^{-1}]

$k_{tm} = k_p \times 1.42 \times 10^{-2}$ exp(-2700/RT) [L mol^{-1} s^{-1}]

$k_{ts} = k_p \times 3.4 \times 10^{-5}$ for t-butyl alcohol [L mol^{-1} s^{-1}]

$k_{ts} = k_p \times 34 \times 10^{-4}$ for toluene [L mol^{-1} s^{-1}]

$k_{td0} = 0$ [L mol^{-1} s^{-1}]

$k_{tco} = 2.7 \times 10^{10}$ exp(−2800/RT) [L mol^{-1} s^{-1}]

$k_{tpo} = k_p \times 7 \times 10^{-3}$ exp(−2700/RT) [L mol^{-1} s^{-1}]

$k_{tp} = k_{tpo}$ exp(−0.282M/S), solution polymerization [L mol^{-1} s^{-1}]

$k_{db} = k_p \times 0.66$ [L mol^{-1} s^{-1}]

B. Free volume theory parameters[29–31]

I. Monomer	$V_m^* \times 10^3$ (m^3 kg^{-1})	$(K_{11}/\gamma) \times 10^6$ (m^3 kg^{-1} K^{-1})	$K_{21} - T_{g1}$ (K)
Vinyl acetate	0.855	1.25	−38.5
II. Solvents	$V_s^* \times 10^3$ (m^3 kg^{-1})	$(K_{12}/\gamma) \times 10^6$ (m^3 kg^{-1} K^{-1})	$K_{22} - T_{g2}$ (K)
t-butyl alcohol	0.967	0.72	−56.6
toluene	0.917	2.20	−102.72
III. Polymer	$V_p^* \times 10^3$ (m^3 kg^{-1})	$(K_{13}/\gamma) \times 10^7$ (m^3 kg^{-1} K^{-1})	$K_{23} - T_{g3}$ (K)
PVAc	0.728	4.33	−258.2

$$D_I = D_{I0} \exp\lfloor -\gamma V_I^* M_{jI}[(\omega_m/M_{jm}) + (\omega_p/M_{jp})]/V_F \rfloor \quad (17)$$

Glass effect

$$\frac{1}{k_p} = \frac{1}{k_{p0}} + \frac{1}{4\pi N_A r_m D_m} = \frac{1}{k_{p0}} + \frac{r_m^2 P_{00}}{3D_m}; r_m = r_t \quad (18)$$

$$D_m = D_{m0} \exp\lfloor -\gamma(\omega_m V_m^* + \omega_p V_p^* \xi_{13})/V_F \rfloor \quad (19)$$

Model parameters

The kinetic mechanism for MMA bulk polymerization includes initiation, transfer to initiator reaction, propagation, termination reactions as well as transfer to monomer. The kinetic parameters, the thermophysical properties as well as the diffusion-controlled reactions parameters for the MMA bulk polymerization are given in full detail elsewhere.[4]

Regarding the free radical polymerization of vinyl acetate polymerization the estimation of kinetic rate parameters has been the subject of extensive experimental investigation as reviewed by Reichert and coworkers.[20–22] In this work, the kinetic rate constants of Hamer and Ray[23–25] were adopted. The values of the kinetic rate constants are summarized in Table I. The thermo-physical properties of the solution constituents are given in standard references.[26–28]

The free volume parameters used in this work for the free radical polymerization of VAc are also summarized in Table I.[31] The parameter ξ [eqs. (11) and (12)] is defined as the ratio of the critical molar volume of the solvent jumping unit to that of the polymer jumping unit. The parameter ξ_{13} (vinyl acetate-PVAc) was set equal to 0.6, the solvent-polymer parameter ξ_{23} was set equal to 0.86 for toluene and equal to 0.97 for t-butyl alcohol according to our previous work.[5,29,30] D'_p0 [eq. (12)] was set equal to 10^{-4} m^2 s^{-1} for simplicity.

Preliminary parameter estimation results reveal the existence of multiple indeterminate parameters regarding the estimated values of transfer to initiator reaction kinetic rate constant (k_r) and the initial amount of species A*. Numerical experimentation has proved that the production rate of species A* could be assumed in absolute value equal to the consumption rate of solvent S or the monomer M in the case of bulk polymerization. This is merely the simplest thing to do, but it has been proved very efficient in simulating our laboratory data.

RESULTS AND DISCUSSION

Test of the isothermal hypothesis

Before proceeding with the study of the effect of several parameters on the polymerization rate data, the isothermal assumption was examined. As previously mentioned, one serious problem associated with the free radical polymerization of vinyl monomers is the production of a large amount of energy (heat) during the course of the reaction. This is especially pronounced with bulk polymerizations in the region of the so-called auto-acceleration, or gel-effect, or Trommsdorff-Norrish effect. Therefore, a significant temperature rise was measured during these polymerizations, questioning the results carried out under isothermal conditions. MMA is such a monomer presenting the autoacceleration effect in a great extent and generating a large amount of heat during polymerization. A number of papers have

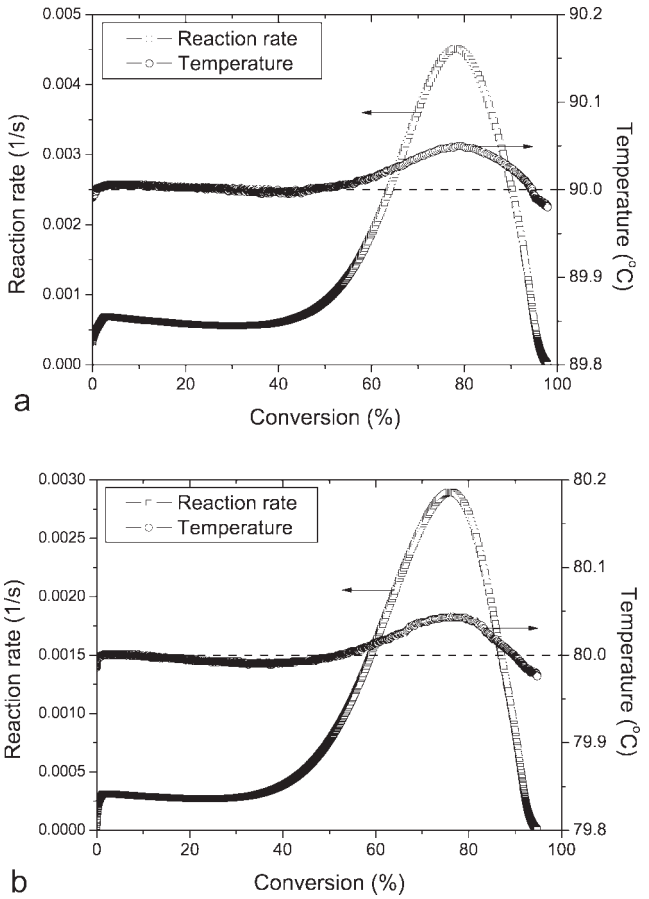

Figure 1 Polymerization rate and reaction temperature versus monomer conversion during bulk polymerization of MMA at 90°C (a) and 80°C (b). $[I]_0 = 0.03M$ AIBN.

been published questioning the isothermal conditions during the reaction.[1] Results on polymerization rate and reaction temperature during synthesis of PMMA at two temperatures 80 and 90°C appear in Figure 1. As it can be seen from this Figure, although the reaction rate increases during autoacceleration by an order of magnitude, the temperature in the reaction medium does not increase more than 0.05°C. Therefore, it can be postulated that DSC is able to keep strictly isothermal conditions during the whole course of polymerization.

MMA bulk polymerization

In this section, results are presented on the bulk polymerization of MMA, a model polymer extensively studied in literature. Kinetic data for this system are readily available in literature from numerous independent investigators.[3,4] Polymerization rate data was collected at different reaction temperatures and initial initiator concentrations. In particular the following set of experiments was carried out.

1. Isothermal bulk polymerization at 0.03*M* initial AIBN concentration and temperatures 60, 70, 80,85, 90, and 95°C and

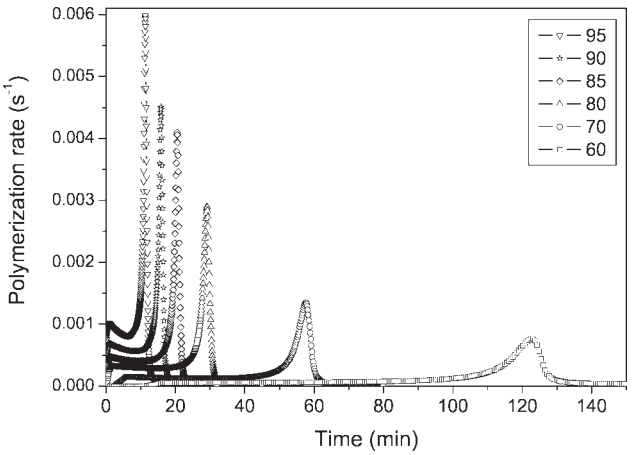

Figure 2 Polymerization rate versus time during bulk polymerization of MMA at different temperatures. $[I]_0 = 0.03M$ AIBN.

2. Isothermal bulk polymerization at 80°C and initial AIBN concentrations of 0.01, 0.03, 0.05, 0.07, and 0.09 mol L^{-1}.

The effect of temperature and initial initiator concentration on the reaction rate variation with time appears in Figures 2 and 3, respectively. As it is expected, an increase in the reaction temperature and the initial initiator concentration results in increased reaction rates. Polymerization lasts for 160 min at 60°C, while only for 15 min at 95°C. Higher reaction temperatures also result in higher final degrees of conversion as well as higher maximum reaction rates, while the final double bond conversion does not seem to depend on the initial initiator concentration. All polymerizations showed a short induction period before the onset of the reaction. The induction period was found to decrease with increasing polymerization temperature and initial

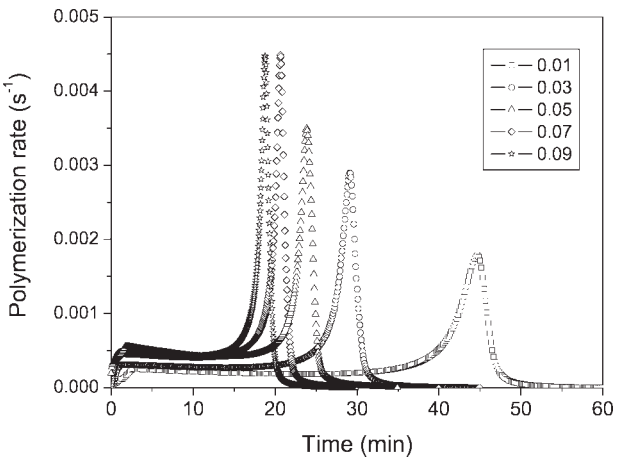

Figure 3 Polymerization rate versus time during bulk polymerization of MMA at different initial initiator concentrations, $T = 80$°C.

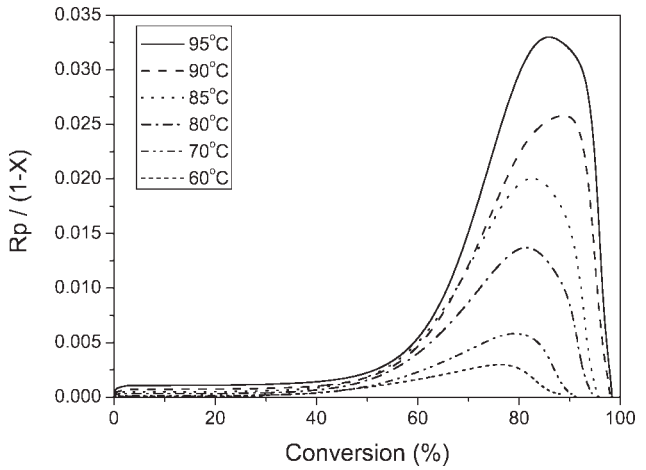

Figure 4 Plot of $R_p/(1-X)$ versus conversion for the free radical polymerization of MMA at different temperatures.

initiator concentration and becomes significant only at the lowest temperature (i.e., 60°C). The induction period appears to be caused by oxygen inhibition of the polymerization caused by small amounts of oxygen encapsulated inside the sealed sample pans. The presence of an inhibition time is sometimes beneficial, as it enables stabilization of the sample temperature in DSC and achievement of a good baseline before the beginning of polymerization.

Subsequently, to show the strong effect of diffusion-controlled phenomena on the reaction kinetics, the polymerization rate, R_p, is plotted as a function of monomer conversion, X, devided over $(1-X)$. A straight line parralel to the x-axis should be obtained by plotting $R_p/(1-X)$ versus conversion or time and by assuming (a) absence of diffusion-controlled phenomena on the propagation and termination rate constants, (b) negligible initiator consumption, (c) the quassi-steady-state approximation is valid. Such a plot appears in Figure 4. As it can be seen, initially a constant value holds for k with increased values with reaction temperature. The point where this line deviates from the initial constant value denotes the onset of diffusion-controlled phenomena. This value ranges from 10 to 12% depending on polymerization temperature and is lower than the corresponding values estimated by other techniques (for example by taking the deviation from linearity of the $-\ln(1-X)$ versus time curve). From Figure 4, it is obvious that diffusion-controlled phenomena have a great influence on polymerization kinetics.

At this point, the overall activation energy of the polymerization reaction can be estimated from the experimental data, according to the following procedure. Combining eqs. (4) and (6) and assuming that the quassi-steady-state approximation and long-chain-hypothesis hold one can arrive to the following equation

$$-\frac{dM}{dt} = k_p M\left(\frac{fk_d[I]}{k_t}\right)^{1/2} \Rightarrow \frac{dX}{dt} = k_p(1-X)\left(\frac{fk_d[I]}{k_t}\right)^{1/2} \tag{20}$$

Equation (20) can be integrated assuming that all kinetic rate constants and initiator efficiency are constant to yield an expression which directly correlates the monomer conversion with an observed overall kinetic rate coefficient, k. It should be noted that eq. (21) is valid only for low degrees of monomer conversion:

$$-\ln(1-X) = k_t \tag{21}$$

with

$$k = k_p\left(\frac{fk_d}{k_t}\right)^{1/2}[I]^{1/2} \tag{22}$$

The overall kinetic rate constant, k can be obtained from the slope of the initial linear part of the plot of $-\ln(1-X)$ versus t. Such plots at conversion values in between 1 and 10% (i.e., $1\% < X < 10\%$) appear in Figure 5. The lowest limit was taken such as to eliminate the inhibition period, while the highest value was well below the onset of diffusion-controlled phenomena. The experimental data fit very well to straight lines at all different temperatures, indicating the validity of eq. (21) in the specific conversion interval.

Considering the temperature dependence of the polymerization rate, it is given by the temperature dependence of the individual rate coefficients. Each rate coefficient follows its own Arrhenious law, $k_i = A_i \exp(-E_i/\mathrm{RT})$, where A_i is the pre-exponential factor and E_i denotes the activation energy. According to the definition of the observed overall kinetic rate coefficient, k [eq. (22)] the overall activation energy

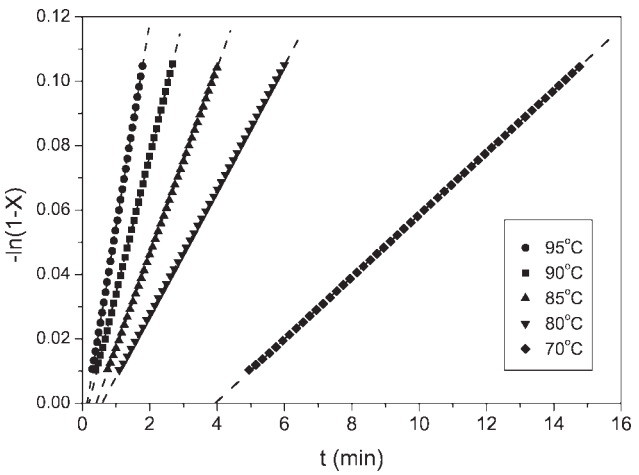

Figure 5 Plot of $-\ln(1-X)$ versus time for the bulk polymerization of MMA at different temperatures.

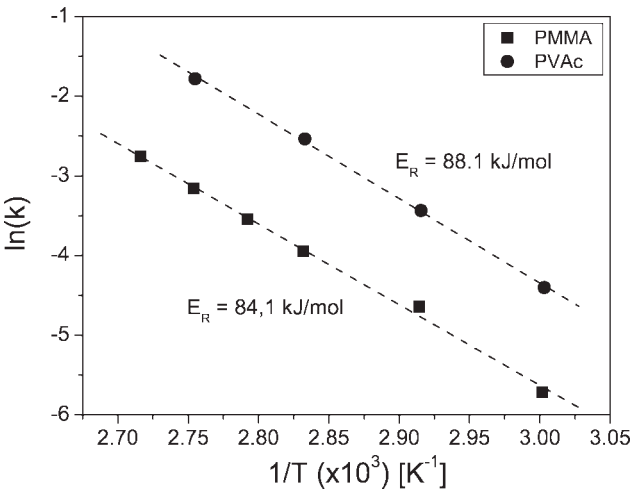

Figure 6 Arrhenius-type plot for the estimation of the overall activation energy during bulk free-radical polymerization of MMA and VAc.

of the polymerization rate, E_R should be given by the activation energies of the elementary reactions, propagation (E_p), initiation (E_i), and termination (E_t), according to:

$$E_R = E_p + \frac{1}{2}(E_i - E_t) \tag{23}$$

Accordingly, from the slope of ln(k) versus $1/T$ the polymerization reaction overall activation energy could be obtained. As it can be seen in Figure 6, all data follow a good straight line with a slope providing an activation energy equal to 84.1 kJ mol^{-1} and an overall kinetic rate coefficient, assuming constant initiator concentration, equal to k′ (L$^{1/2}$ mol$^{-1/2}$ s^{-1}) = 5.2 10^9 exp(-84,100/RT). This values of E_R is very close to the literature values 84.9,[32] 85.5,[33] 83.1,[34] and 82.6[35] kJ mol^{-1}.

Furthermore, the aim of this work is to further validate the model developed in our previous studies[1–5] as briefly described in the previous section. For this purpose, a comparison of model predictions with the DSC and molecular weight experimental data is made in this work. Model parameters were estimated by a general nonlinear regression package, GREG[36] that uses as its objective function minimization of the sum of squares of the differences between the experimental conversion versus time data from DSC and that predicted from the solution of the system of differential equations. GREG developed by Caracotsios, Stewart, and Sorensen in the University of Wisconsin, Madison, is a nonlinear parameter estimator that uses a Bayesian approach to estimate model parameters and their inference intervals and covariances, using single-response or multiresponse data. Because of its local optimization, GREG is a very fast routine. This is the main reason why GREG was chosen to optimize the rate parameters in the kinetic model. The model needs to be solved repetitively in every iteration of the optimization process, so the speed of the optimization is crucial.

In our simulations, the initial induction time due to the possible existence of oxygen traces, which also act as inhibitor, was neglected as preliminary simulations indicate that one could not get independent estimates for both the initial concentrations of oxygen or other species causing inactivation of initiator and the respective kinetic rate constants.

As linear polymers are produced by the MMA bulk polymerization, the simplified version of the model for the gel effect was utilized as described in our previous work.[4] This simplified model is directly derived by the eqs. (7)–(19) by setting the solvent and the branched radical concentrations equal to zero. However, the model accounts not only for the gel effect but also for the cage and glass effects as well as for the residual termination.

This model includes as adjustable parameters, the diffusion quantities D_{p0}, the cage effect parameter (E/D_{l0}), the glass effect parameter (D_{m0}), the transfer to initiator reaction kinetic rate constant (k_r) as well as the residual termination parameter A_r. In our previous study,[4] the effect of process conditions on the polymerization process and product quality was thoroughly studied. This study focuses on the effect of polymerization conditions on the values of estimated parameters.

The simulated DSC data include a complete parametric analysis for initial initiator concentration and polymerization temperature. The experimental conditions and the estimated parameters obtained in this work together with those reported previously,[4] are summarized in Table II. Representative results indicating a fairly good fitting for MMA bulk polymerization are illustrated in Figures 7 and 8. To quantify the accuracy of the fitting procedure some statistical parameters were estimated and are reported in Table III. As it can be seen, in all different cases the square of the correlation coefficient is larger than 0.991 meaning a rather good fitting of the model to the experimental data. Moreover, as shown in Table IV, the estimated values of the average molecular weights are in satisfactory agreement with the experimental measured data further validating our model.

More specifically, both the polymerization temperature and the initial initiator concentration have moderate effect on both the free volume proexponential factor (D_{p0}) and the residual termination parameter A_r. For both parameters (D_{p0} and A_r) almost constant values (D_{p0} = 0.031 ± 0.017 cm^2 s^{-1}, A_r = 35 ± 10), as predicted by the model, are shown in Table II. The slight decrease in free volume proexponential factor (D_{p0}) with increasing polymerization

TABLE II
Estimated Parameters for MMA Bulk Polymerization

Polymerization conditions T (°C); $[I]_0$ (gmol L^{-1})		D_{p0} (cm^2 sec^{-1})	D_{m0} (cm^2 sec^{-1})	E/D_{I0} (sec cm^{-2})	A_r	k_r (L mol^{-1} s^{-1})
60	0.03	0.049	7.9×10^{-10}	0.01	25.1	0.7
70	0.03	0.029	8.2×10^{-8}	0.053	73.3	0.19
70	0.0155[4]	0.06	1×10^{-8}	2.66	14.1	–
70	0.0258[4]	0.042	1.3×10^{-9}	47.86	31.21	–
80	0.01	0.034	3.45×10^{-7}	6.93×10^{-3}	35.15	2.3×10^{-3}
80	0.03	0.023	7.9×10^{-7}	0.07	38.1	0.2
80	0.05	0.020	6.6×10^{-7}	0.069	39.7	0.2
80	0.07	0.017	2.93×10^{-7}	0.082	36.2	0.22
80	0.09	0.016	6.2×10^{-7}	0.097	29.2	0.31
85	0.03	0.019	1.76×10^{-6}	0.073	32.8	0.19
90	0.03	0.018	6.7×10^{-5}	0.016	34.7	0.24
90	0.0155[4]	0.019	2.2×10^{-6}	7.6	38.7	–
90	0.0258[4]	0.014	4.4×10^{-7}	2239	22.1	–
95	0.03	0.013	3.7×10^{-5}	0.0015	44.7	0.021

temperature or initial initiator concentration could be attributed to the fact that this parameter also includes the effect of the segmental diffusion of the radical chains. This is done by multiplying the self-diffusion coefficient by a factor F_{seg}.[3,4] The effect of temperature on F_{seg} could explain the slight shift in the value of this parameter (D_{p0}).

The slight variation in the value of residual termination parameter (A_r) with temperature is attributed to the profound effect of the temperature on the propagation rate constant (k_p), which is also incorporated in the equation describing the residual termination [eq. (9)]. This profound effect causes a slight decrease in the estimated value of residual termination parameter (A_r) to account for the residual termination phenomenon. However, the initial initiator concentration has little effect on the residual termination parameter (A_r) and this parameter has an almost constant value (33 ± 3) as predicted by our model. Please, note that the estimated values for these parameters (D_{p0} and A_r) are very close to the reported values in our previous work[4] which are also shown in Table II.

The initial initiator concentration has little effect on the glass effect parameter (D_{m0}), which has an almost constant value ($5.5 \pm 2.53 \times 10^{-7}$) as predicted by our model.[1–4] However, polymerization temperature has a profound effect on this parameter which sharply increases by increasing the temperature as shown in Table II.

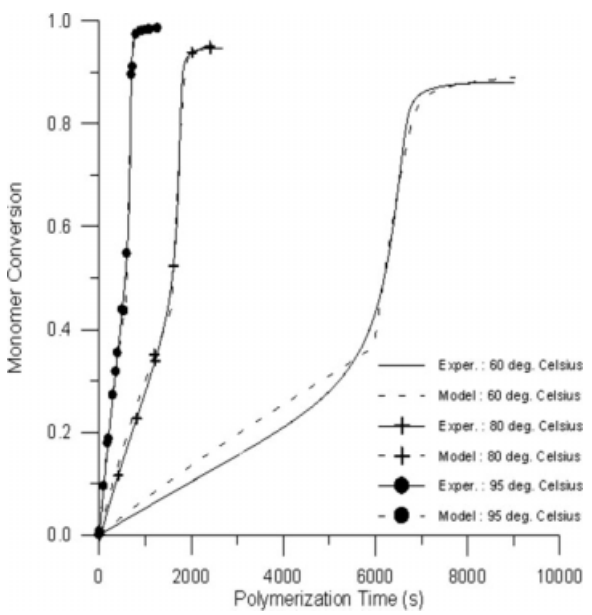

Figure 7 Comparison of model predictions for monomer conversion with experimental data for MMA bulk polymerization. $[I]_0 = 0.03M$ AIBN.

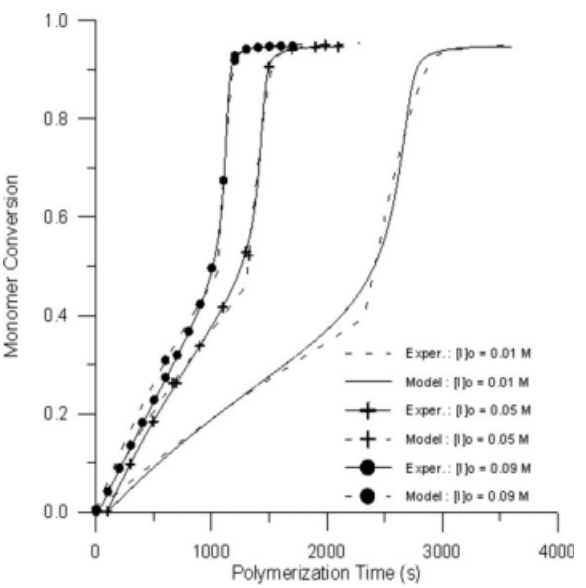

Figure 8 Comparison of model predictions for monomer conversion with experimental data for MMA bulk polymerization. Polymerization temperature: 80°C.

TABLE III
Statistical Parameters from the Fitting Procedure

Polymerization conditions		Sum of squares	Square of the correlation coefficient, R^2
Temperature (°C)	$[I]_0$ (M)		
A. MMA bulk polymerization			
70	0.03	0.411	0.9945
80	0.03	0.272	0.9944
85	0.03	0.104	0.9962
90	0.03	0.078	0.9964
95	0.03	0.070	0.9963
80	0.01	0.159	0.9963
80	0.05	0.165	0.9962
80	0.07	0.111	0.9964
80	0.09	0.188	0.9923
B. VAc bulk polymerization			
60	0.03	0.0845	0.9905
70	0.03	0.0823	0.9984
80	0.03	0.0236	0.9966
C. VAc solution polymerization (solvent : t-butyl alcohol)			
60	0.1	1.120	0.9945
D. VAc solution polymerization (solvent : toluene)			
70	0.1	0.513	0.9987

This behavior is expected as the polymerization temperature in all experiments is very close to the glass transition temperature of the reactant mixture. Therefore, glass transition occurs during polymerization at different instances causing a large variation of the glass effect parameter (D_{m0}). Similar effects for the polymerization temperature on this parameter were also found in our previous work[4] as shown in Table II.

Regarding the cage-effect parameter (E/D_{i0}) the estimated values in this work are significantly smaller than in our previous study due to the addition of the transfer to initiator reaction kinetic rate constant as an adjustable parameter. More specifically, a significant part of the cage effect could be attributed to the transfer to initiator reaction kinetic rate constant introduced in this work to account for the absence of stirring and the possible presence of inhibitors (oxygen) in the DSC experiments. Therefore, the effect of oxygen or other species causing deactivation of initiator could explain the large variation of both parameters (E/D_{i0},k_r) summarized in Table II.

Vinyl acetate bulk polymerization

In this section, polymerization resulting in branched polymers was investigated. As a model polymer in this category, the polymerization of VAc with AIBN initiator was studied. Results on the effect of temperature on polymerization rate appear in Figure 9. Again an increase in temperature promotes the reaction, which is completed at 15 min at 90°C compared to more than 100 min at 60°C. The overall activation energy of the polymerization was estimated according to the process described in the previous section and a plot of ln(k) versus $1/T$ is included in Figure 6. As it can be seen, all data follow a good straight line with a slope providing an activation energy equal to 88.1 kJ mol^{-1}. By using eq. (23) with values taken from Table I, i.e., $E_p = 6.3$ kcal mol^{-1}, $E_i = 30$ kcal mol^{-1} and $E_t = 2.7$ kcal mol^{-1}, the E_R is calculated to be 20 kcal mol^{-1} = 83.6 kJ mol^{-1} a value comparable to the experimentally estimated. Concerning the isothermal hypothesis discussed in "Test of the isothermal Hypothesis" section in the case of MMA polymerization, it could be postulated that the same behavior is expected during VAc polymerization since the maxima in the reaction rates are similar (i.e., 0.0045 and 0.003 s^{-1} for MMA and VAc, respectively) and the total amount of heat released, $\Delta H_0 \times R_p$, is also similar (the maximum values are $55 \times 0.0045 = 0.24$ kJ mol^{-1} s^{-1} and $88 \times 0.003 = 0.26$ kJ mol^{-1} s^{-1}, for MMA and VAc, respectively).

The model for the VAc bulk polymerization includes as adjustable parameters the initiator efficiency f_0, the diffusion quantity α, the cage effect parameter (E/D_{i0}) as well as the residual termination parameter A_r [eq. (9)]. Preliminary results indicate that the transfer to initiator reaction kinetic rate constant (k_r) and the free volume parameter (D_{p0}) are indeterminate parameters (one could not get

TABLE IV
Comparison Between Experimental and Predicted Average Molecular Weights for MMA Bulk Polymerization

$[I]_0$ (M)	Polymerization temperature (°C)	Number average MW (experiment)	Number average MW (model)	Weight average MW (experiment)	Weight average MW (model)
0.03	60	345,460	348,330	1.5208E6	1.9602E6
0.03	70	255,680	216,900	894,880	714,020
0.03	80	171,070	126,950	426,370	513,800
0.03	85	99,680	100,500	339,230	423,100
0.03	90	80,130	76,300	228,340	318,300
0.03	95	78,540	58,300	196,350	216,100
0.01	80	282,460	239,900	662,400	923,500
0.05	80	115,410	92,263	286,410	372,440
0.07	80	74,700	74,789	295,980	312,500

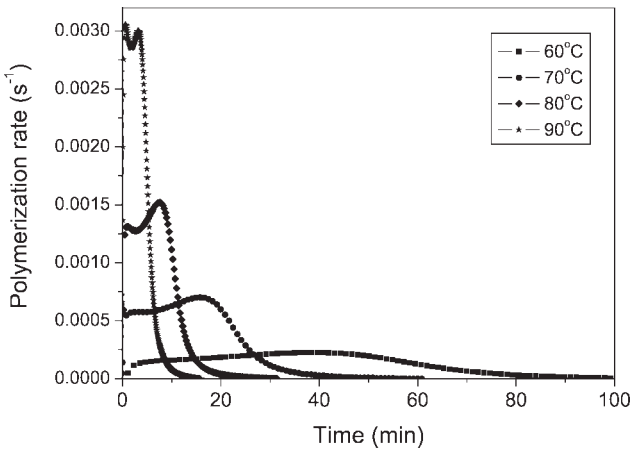

Figure 9 Bulk polymerization of vinyl acetate. Effect of temperature on polymerization rate. $[I]_0 = 0.03M$ AIBN.

independent values). The parameter D_{p0} was assumed to have a constant value equal to 2×10^{-10} cm^2 s^{-1}. The glass effect was also considered by setting the value of the respective parameter (D_{m0}) equal to 10^{-4} cm^2 s^{-1}, which is a typical value accounting for the diffusion of small molecules, such as the VAc molecules, in rubbery polymers.

The simulated DSC data by nonlinear regression analysis includes one initial initiator concentration (AIBN, $[I]_0 = 0.03M$) for three different polymerization temperatures. A fairly good fitting is depicted in Figure 10. The estimated parameters as well as the polymerization conditions are summarized in Table V. There is slight decrease in the value of the residual termination parameter A_r (see Table V) with temperature similar to the observed variation in

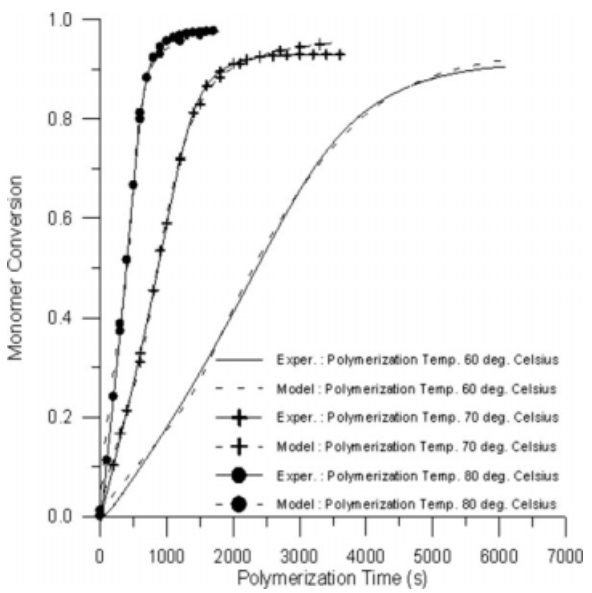

Figure 10 Bulk polymerization of vinyl acetate. Comparison of model predictions for monomer conversion with experimental data. $[I]_0 = 0.03M$ AIBN.

TABLE V
Estimated Parameters for the VAc Bulk Polymerization

Polymerization temperature	f_0 (AIBN)	α	A_r	E/D_{I0} (s cm^{-2})
60°C	0.0785	3.9×10^{-3}	185.7	10.05
70°C	0.141	3.7×10^{-3}	151	45.49
80°C	0.256	3.21×10^{-3}	92.2	137.4

Table II for the MMA polymerization. This could also be attributed to the profound effect of polymerization temperature on k_p as already discussed in the previous subsection. The diffusion parameter α has an almost constant value in the range $3.35 \pm 0.35 \times 10^{-3}$ as predicted by the theory.[5] The slight variation with temperature could be attributed to the fact that this parameter also includes the effect of the segmental diffusion of the radical chains by multiplying the self-diffusion coefficient by a factor F_{seg}.[3,4] The effect of temperature on the factor F_{seg} could explain the slight variation of the diffusion parameter α with temperature.

The initiator efficiency f_0, is in the range 0.07–0.26 while the cage-effect parameter (E/D_{i0}) has significantly greater values than the estimated ones in this work for the MMA polymerization due to the fact that the transfer to initiator reaction kinetic rate constant (k_r) was not included in the estimation procedure as adjustable parameter (please, see discussion in the previous sub-section). However, this parameter has values close to the estimated ones for the bulk MMA polymerization as obtained in our previous work[4] (see Table II). This further validates our model since in both experiments (MMA and VAc bulk polymerization) the same type of initiator (AIBN) was used.

Regarding the possible estimation of MW at the end of polymerization as in the case of MMA polymerization, preliminary simulations indicate (see Fig. 11) the formation of polymer structure with extremely high values of weight average molecular weight and polydispersity due to transfer to polymer and propagation on terminal double bond reactions. These reactions along with the termination by combination reaction could lead to the formation of a gel phase near the end of the DSC experiment through sol-gel transition at very high monomer conversion. Experimental MW data obtained at the end of the reaction for both bulk and solution polymerization of VAc indicate the existence of a liquid phase with very low polydispersity (~2.5) due to the possible sol-gel transition near the end of the DSC experiment (formation of a gel phase incorporating the branched polymer and a sol phase with polymer having low polydispersity values). Therefore, preliminary simulations were run to detect the onset of this sol-gel transition and exclude this part of the

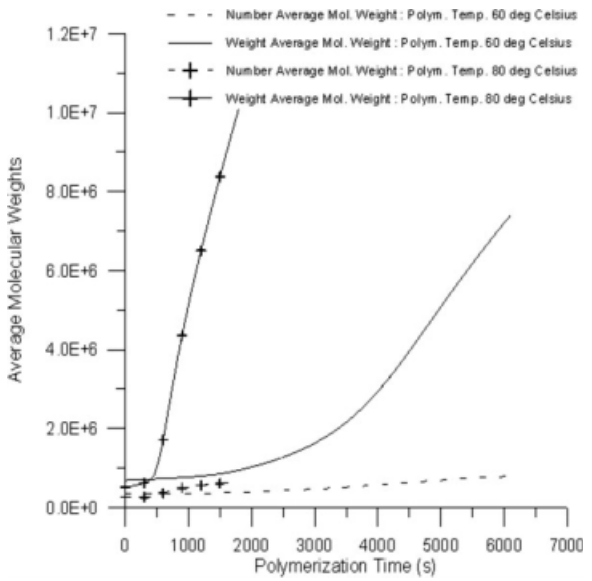

Figure 11 Bulk polymerization of vinyl acetate. Model predictions for "dead" polymer average molecular weights. $[I]_0 = 0.03M$ AIBN.

experimental data from the parameter estimation procedure.

Vinyl acetate solution polymerization

Differential scanning calorimetry could also be applied in monitoring polymerization reactions taking place in solution. As such, the solution polymerization of vinyl acetate was investigated in two different solvents, namely toluene and t-butanol. The effect of the amount of solvent on the polymerization rate and double bond conversion during solution polymerization of VAc in t-butanol and toluene appear in Figures 12 and 13, respectively.

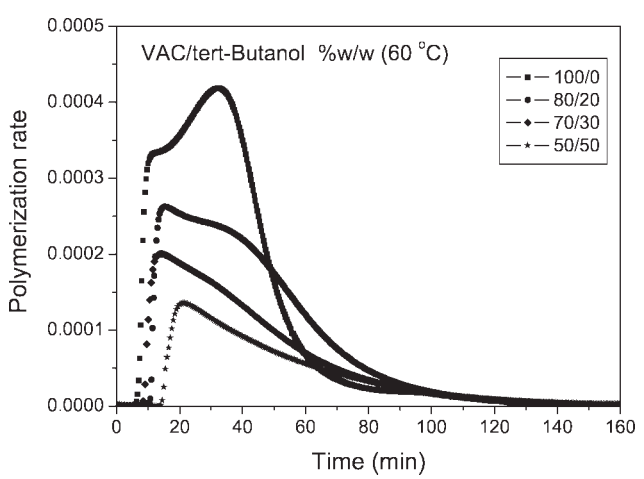

Figure 12 Solution polymerization of VAc in t-butanol at 60°C. Effect of the initial solvent concentration on polymerization rate. $[I]_0 = 0.1M$ AIBN.

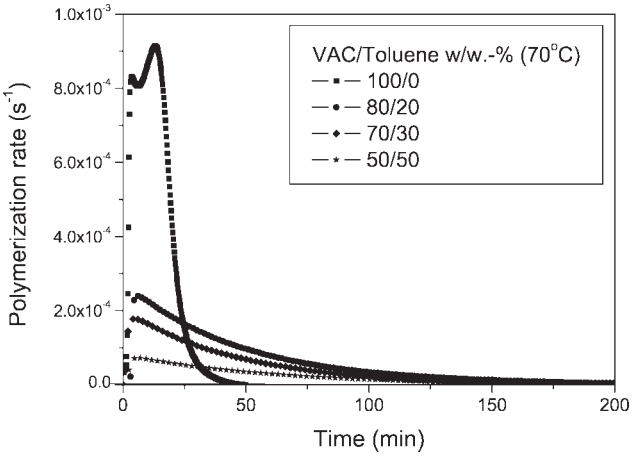

Figure 13 Solution polymerization of vinyl acetate in toluene at 70°C. Effect of the initial solvent concentration on polymerization rate. $[I]_0 = 0.1M$ AIBN.

It can be seen that as the amount of solvent is increased the gel-effect is suppresed the reaction rate is greatly lowered and the reaction lasts longer with lower degrees of conversion. An important point here is that as most solvents used are volatile, great care shoud be taken to carry out the reaction at temperatures substantially lower than the boiling point of the solvent during solution polymerization otherwise possible solvent evaporation could take place altering the mass of the sample and the precision of the results.

The model for the VAc solution polymerization includes as adjustable parameters the initiator efficiency f_0, the diffusion quantities D_{p0} and α, the transfer to initiator reaction kinetic rate constant (k_r) as well as the residual termination parameter A_r. The cage effect and the glass effects were considered minimal due to the presence of a solvent.

The estimated adjustable parameters by fitting the conversion data as obtained by DSC experiments are given in Table VI. The resulting fitting is illustrated in Figures 14 and 15. In Table VI the adjustable parameters obtained in our previous work[5] by using data from Chatterjee et al.[7] (well stirred reactor at 60°C, initial t-butyl concentration: 16–36% (w/w), AIBN initial conc.: $4.2 \times 10^{-4} - 1.6 \times 10^{-3}$ M) are also summarized. The current DSC experiments were carried out at the same temperature without using any stirring. The initial t-butyl alcohol concentration in the DSC experiments is in the range 30–50% (w/w) and considerably higher initial AIBN concentration (0.1M) was used.

Estimated parameters from our previous work[5] by fitting McKenna and Villanueva[8] data (well stirred reactor at 60°C, initial toluene conc.: 60–90% (w/w), AIBN intial conc.: 0.004 mol/lt) is also reported in Table VI. In this work, a slightly different polymerization temperature was used (70°C) in the DSC

TABLE VI
Estimated Parameters for the VAc Solution Polymerization

System	f_0 (AIBN)	D_{p0} (cm^2 sec^{-1})	α	A_r	k_r (L mol^{-1} s^{-1})
Toluene/VAc					
Previous work[5]	1.8×10^{-4}	1.14×10^{-10}	0.018	–	–
This work	7.94×10^{-4}	2.18×10^{-10}	0.069	97.72	0.04
t-Butyl alcoh./VAc					
Previous work[5]	0.1	3.98×10^{-9}	0.007	562.3	–
This work	0.013	1.94×10^{-10}	0.0075	239.8	1

experiments while the initial initiator concentration was considerably higher (0.1*M*) and the initial toluene concentration varies from 20–50 % (w/w)

The estimated initiator efficiency (f_0) in this study was found to be in the same order of magnitude that reported in our previous work[5] for the vinyl acetate -polymerization in toluene. However, estimated initiator efficiency for the solution polymerization of VAc in t-butyl alcohol is one order of magnitude below that reported in our previous work. This discrepancy in the estimated initiator efficiency could be attributed to the different experimental conditions. More specifically, the small values of initiator efficiency shown in Table II for both solvents could be attributed to the absence of stirring in the DSC experiments or to the presence of oxygen traces consuming initiator during the incubation period. Both effects are well established in the literature for vinyl polymerizations[37] and explain the increased values of initial initiator concentration (0.1*M*) used in this work.

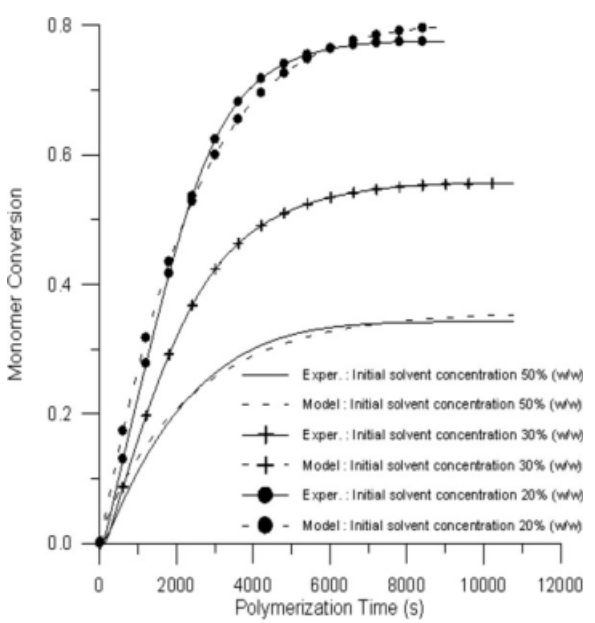

Figure 14 Solution polymerization of vinyl acetate in t-butyl alcohol at 60°C. Comparison of model predictions for monomer conversion with experimental data. $[I]_0$= 0.1*M* AIBN.

However, the estimated initiator efficiency has larger values for the current DSC data than for the well stirred experiments of Mckenna and Villanueva.[8] This discrepancy could be explained by the fact that the reported data in our previous work[5] is for the low conversion range while in this work the whole conversion range was considered. Another possible source of this descrepancy is the slightly different polymerization temperature (60°C in Mckenna and Villanueva[8] experiments vs. 70°C in this work) or the different initial solvent concentration. It should be noted here that the difference in polymerization temperature is anticipated to have moderate effects on the initiator efficiency as shown on the previous subsection for VAc bulk polymerization.

Although completely different experimental conditions were used, the gel effect parameters (D_{p0} and α and A_r), as shown in Table VI, are in the same order of magnitude with the reported ones in our previous work[5] as well as with the obtained ones in the previous part for the bulk polymerization of VAc. The differences between this work and our previous work concerning the data for the gel effect parameter could be attributed to the different experimental

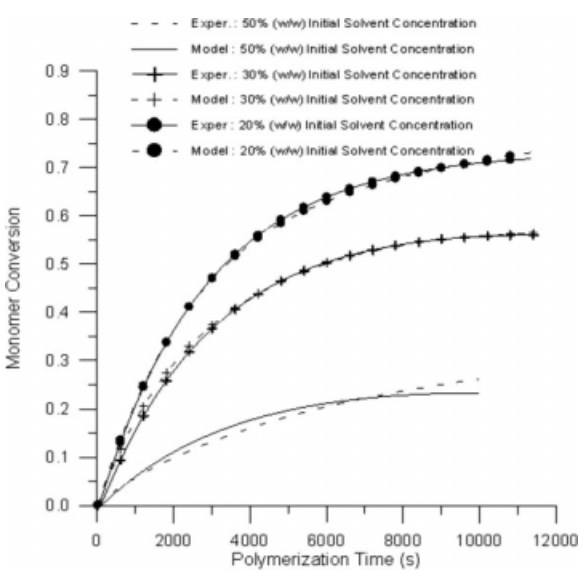

Figure 15 Solution polymerization of vinyl acetate in toluene at 70°C. Comparison of model predictions for monomer conversion with experimental data. $[I]_0$= 0.1*M* AIBN.

conditions used in this work regarding initial initiator and solvent concentrations.

However, the model shoes good ability in simulating experimental data by using different initial initiator and solvent concentrations, in the presence or absence of stirring for both linear or branched polymers. This fact further validates both the developed experimental procedures and the model applied in this work.

CONCLUSIONS

In this work, free radical polymerization reactions producing linear or branched polymers and governed by diffusion-controlled phenomena were both experimentally and theoretically studied in the absence or presence of a solvent (i.e., bulk or solution polymerization). As case-studies the bulk polymerization of MMA and VAc were investigated as well as the solution polymerization of VAc with different solvents. Reaction rate and fractional monomer conversion was measured by DSC at different experimental conditions and the data were successfully simulated by using a model based on sound principles such as the free volume theory. The estimated parameters of this model were found to be in close agreement with those reported in literature, thus validating both the experiments and models used in this work. It is believed that this work might contribute to a more rational design of polymerization reactors.

George Verros thanks Ms Kate Somerscales for her help in preparing the manuscript.

NOMENCLATURE

A*, A^*	Species responsible for initiator deactivation; its concentration
A_r	Residual termination adjustable parameter
$D_{n,b}$; $D_{n,b}$	"Dead" polymer having n monomer units and b number of branches; its concentration
D_s; D_s	"Dead" polymer having s monomer units (sum of species with different degree of branching); its concentration
D_{I0}	Free volume theory proexponential parameter for initiator fragment self-diffusion
D_{m0}	Free volume theory proexponential parameter for monomer self-diffusion
D_{p0}; D_{p0}'	Free volume theory proexponential parameter
$\overline{D}_{p,0}$	Self-diffusion coefficient of linear "live" radicals
$\overline{D}_{p,br}$	Self-diffusion coefficient of "live" radicals having different degree of branching
E/D_I	Cage effect parameter
f	Initiator efficiency
j_c	Entanglement spacing
I; I	Initiator; its concentration
k_d	Initiator decomposition kinetic rate constant
k_{db}	Terminal double-bond reaction kinetic rate constant
k_{t0}	Intrinsic termination rate constant defined at zero conversion and involving two short chains
k_{tm}	Chain transfer to monomer kinetic rate constant
k_{tp}	Chain transfer to polymer kinetic rate constant
k_{ts}	Chain transfer to solvent kinetic rate constant
k_p	Propagation rate kinetic rate constant
k_r	Transfer to initiator reaction kinetic rate constant
k_{tc}	Termination by combination kinetic rate constant
k_{td}	Termination by disproportionation kinetic rate constant
K_{1i}	Free volume parameter
K_{2i}	Free volume parameter
M; M	Monomer; its concentration
M_j	Molecular weight
N_A	Avogadro number
P_{00}^T	Total concentration of "live" radicals
P_{0b}	Total concentration of "live" radicals with branches
P_{0l}	Total concentration of linear "live" radicals
$P_{n,b}$; $P_{n,b}$	"Live" polymer having n monomer units and b number of branches; its concentration
PR^*; PR^*	Primary radical from the fragmentation of the initiator; its concentration
r_t	Effective termination reaction radius
r_2	Initial hydrodynamic volume of the polymer,
r_1	Diameter of monomer molecule
R	Universal gas constant
S; S	Solvent agent; its concentration
t	Time
T	Temperature
T_G	Glass transition temperature
V	Reactor volume
V_F	Specific free volume
$\mathbf{V_i^*}$	Specific critical hole free volume of the i-th substance
x_{c0}	Critical degree of polymerization for entanglement of pure polymer
X	Fractional monomer conversion
$\overline{X}_b$	Number average degree of polymerization of the branched "live" radicals.

$\overline{X}_{lr}$ Number average degree of polymerization of the linear "live" radicals

Greek symbols

- α Free volume theory adjustable parameter
- γ Overlap factor
- δ Average root-mean-square end-to-end distance per square root of the number of monomer units in a chain
- τ Auxiliary parameter
- φ_p Volume fraction of polymer
- ω Weight fraction

Subscripts

- *b* Number of long-chain branches in a polymer chain
- *I* Initiator
- *m* Monomer
- *n* Number of monomer units in the polymer chain
- *o* Initial conditions
- *p* Polymer
- *s* Solvent

Superscripts

- = Terminal double bond incorporated into a macromolecule

References

1. Achilias, D. S. Macromol Theory Simul 2007, 16, 319.
2. Achilias, D. S.; Kiparissides, C. J Appl Polym Sci 1988, 35, 1303.
3. Achilias, D. S.; Kiparissides, C. Macromolecules 1992, 25, 3739.
4. Verros, G. D.; Latsos, T.; Achilias, D. S. Polymer 2005, 46, 539.
5. Verros, G. D.; Achilias, D. S. J Appl Polym Sci 2009, 111, 2171.
6. Balke, S. T.; Hamielec, A. E. J Appl Polym Sci 1973, 17, 905.
7. Chatterjee, A.; Kabra, K.; Graessley, W. W. J Appl Polym Sci 1977, 21, 1751.
8. Mckenna, T. F.; Villanueva, A. J Polym Sci Part A: Polym Chem 1999, 37, 589.
9. Regenass, W. Thermochim Acta 1985, 95, 351.
10. Guldbæk Karlsen, L.; Villadsen, J. Chem Eng Sci 1987, 42, 1165.
11. Moritz, H.U. In Polymer Reaction Engineering; Reichert, K. H., Geiseler, W., Eds.; Verlag Chemie: Weinheim, Germany, 1989, p 248.
12. Schmidt, C.-U.; Reichert, K.-H. Chem Eng Sci 1989, 43, 2133.
13. Schuler, H.; Schmidt, C.-U. Chem Eng Sci 1992, 47, 899.
14. Urretabizkaia, A.; Sudol, E. D.; El-Aasser, M. S.; Asua, J. M. J Polym Sci Part A: Polym Chem 1993, 31, 2907.
15. De Buruaga, I. S.; Echevarría, A.; Armitage, P. D.; De La Cal, J. C.; Leiza, J. R.; Asua, J. M. AIChE J 1997, 43, 1069.
16. Santos, A. M.; Févotte, G.; Othman, N.; Othman, S.; Mckenna, T. F. J Appl Polym Sci 2000, 75, 1667.
17. Kemmere, M. F.; Meuldijk, J.; Drinkenburg, A. A. H.; German, A. L. J Appl Polym Sci 2001, 79, 944.
18. Elizalde, O.; Azpeitia, M.; Reis, M. M.; Asua, J. M.; Leiza, J. R. Ind Eng Chem Res 2005, 44, 7200.
19. Konstadinidis, K.; Achilias, D. S.; Kiparissides, C. Polymer 1992, 33, 5019.
20. Baade, W.; Moritz, H. U.; Reichert, K. H. J Appl Polym Sci 1982, 27, 2249.
21. Taylor, T. W.; Reichert, K. H. J Appl Polym Sci 1985, 30, 227.
22. Reichert, K. H.; Moritz, H.-U. Makromol Chem Macromol Symp 1987, 10, 57.
23. Hamer, J. W.; Akramov, T. A.; Ray, W. H. Chem Eng Sci 1981, 36, 1987.
24. Hamer, J. W.; Ray, W. H. Chem Eng Sci 1986, 41, 3083.
25. Hamer, J. W.; Ray, W. H. Chem Eng Sci 1986, 41, 3095.
26. Dean, J. A. Lange's Handbook of Chemistry, 11th ed.; McGraw-Hill: New York, 1973.
27. Perry, R. H.; Green, D. Perry's Chemical Engineers' Handbook, 6th ed.; McGraw Hill: New York, 1984.
28. Wen, J. In Polymer Data Handbook; Mark, J. E., Ed.; Oxford University Press: New York, 1999; p 882.
29. Verros, G. D.; Papachristou, S.; Prinos, J.; Malamataris, N. A. Chem Eng Commun 2003, 190, 334.
30. Verros, G. D. J Membr Sci 2009, 328, 31.
31. Hong, S.-U. Ind Eng Chem Res 1995, 34, 2536.
32. Armitage, P. D.; Hill, S.; Johnson, A. F.; Mykytiuk, J.; Turner, J. M. C. Polymer 1988, 29, 2221.
33. Bauduin, G.; Pietrasanta, Y.; Rousseau, A.; Granier-Azema, D. Eur Polym J 1992, 28, 923.
34. Feliu, J. A.; Sottile, C.; Bassani, C.; Ligthart, J.; Maschio, G. Chem Eng Sci 1996, 51, 2793.
35. Maschio, G.; Bello, T.; Scali, C. Chem Eng Sci 1994, 49, 5071.
36. Caracotsios, M.; Stewart, W. E.; Sorensen, J. P. GREG, General Regression Software for Non-linear Parameter Estimation, User's Manual;Department of Chemical Engineering, University of Wisconsin: Madison, WI, 1986.
37. Luft, G.; Bitsch, H.; Seidl, H. J Macromol Sci Chem 1977, 111, 1089.